Available online at www.sciencedirect.com
SCIENCE DIRECT®
ELSEVIER
Sensors and Actuators A 122 (2005) 317–325
SENSORS AND ACTUATORS A PHYSICAL
www.elsevier.com/locate/sna

Electrically coupled MEMS bandpass filters Part II. Without coupling element

Siavash Pourkamali, Farrokh Ayazi *

School of Electrical and Computer Engineering, Georgia Institute of Technology, 791 Atlantic Drive, Atlanta, GA 30332-0250, USA

Received 30 April 2004; accepted 9 March 2005
Available online 3 May 2005

Abstract

This paper, the second of two parts, introduces electrostatic coupling of micromechanical resonators for implementation of high-order narrow-bandwidth bandpass filters. The concept of electrostatic coupling of closely spaced microresonators and its electromechanical modeling is presented. Electrostatic coupling of resonators does not require any distinct physical coupling elements. The electrostatic coupling strength between the resonators is sharply dependant on the applied polarization voltages to the resonators. Hence the coupling strength and consequently filter bandwidth can be tuned over a wide range after fabrication. It is shown that electrostatic coupling provides the highest degree of tunability and design flexibility among the available microresonator coupling approaches. Low frequency single crystal silicon prototypes of second order electrostatically coupled filters are fabricated and characterized. Filter quality factor as high as 6800 (0.015% BW) with more than one decade of bandwidth tunability is demonstrated for a second order electrostatically coupled beam filter at center frequency of 170 kHz.
© 2005 Elsevier B.V. All rights reserved.

Keywords: Micromechanical filter; Microresonator; Electrostatic coupling; SOI; Quality factor

1. Introduction

In Part I of this paper, electrical coupling of micromechanical resonators for filter synthesis using active and passive electrical coupling elements [1] was presented. It was shown that electrical coupling of microresonators, in addition to having a greater potential for extension into the ultra-high frequency (UHF) range, provides superior tunability and design flexibility compared to the traditionally used mechanical-based approach [2–7].

In this part, the electrostatic coupling approach for implementation of bandpass filters [8] is presented. Electrostatic coupling is an electrical-based passive coupling technique that does not require any distinct coupling elements. In this approach, closely spaced resonators are coupled by the electrostatic forces in between their resonating bodies and result in a higher order resonant system. The coupling strength between the resonators sharply depends on the DC polarization voltage difference between them and can be widely tuned after fabrication. Compared to the previously reported capacitive coupling approach [1], the electrostatic coupling provides even more tunability and design flexibility and alleviates some of the issues associated with capacitive coupling (such as DC biasing of the coupling capacitor).

Electromechanical modeling and derivation of the electrical equivalent circuit for clamped–clamped beam electrostatically coupled filter arrays are presented. Low frequency prototypes of second order electrostatically coupled filters are fabricated and characterized. The validity and precision of the derived electromechanical model is verified by comparing the measured data to the theoretically calculated values and simulation results.

2. Electrostatic coupling

Fig. 1 shows the schematic diagram of an electrostatically coupled beam filter array comprised of a number of resonators

* Corresponding author. Tel.: +1 404 894 9496; fax: +1 404 385 6650.
E-mail addresses: siavash@ece.gatech.edu (S. Pourkamali), ayazi@ece.gatech.edu (F. Ayazi).

0924-4247/$ – see front matter © 2005 Elsevier B.V. All rights reserved.
doi:10.1016/j.sna.2005.03.039

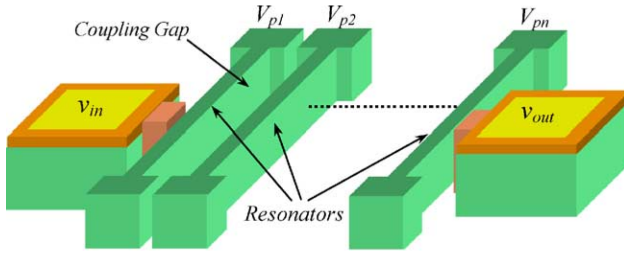

Fig. 1. Schematic diagram of an electrostatically coupled beam filter array.

separated by narrow coupling gaps in between every two adjacent ones.

Application of different DC polarization voltages (V_p) to the adjacent resonators results in an electrostatic force between the two resonant structures attracting them towards each other. As the resonators resonate, the attracting electrostatic force changes by fluctuations of the coupling gap between the two bodies (increases as they get closer to each other and vice versa). Therefore in addition to its static DC value, the electrostatic force has a displacement dependant component. The displacement dependant component can be modeled as a spring in between the two resonators in the mechanical domain. However since the direction of the displacement dependant force component is opposite to the force applied by a mechanical spring, the electrostatic imaginary spring has a negative effective value.

For analytical derivation of the electrostatic force values and coupling strength between the two resonators, assume two closely spaced clamped–clamped beam resonators biased at different polarization voltages. The electrostatic force is distributed along the beam lengths. Dividing each beam into small elements of length dx each, as shown in Fig. 2, the electrostatic force in between each pair of corresponding adjacent elements on the two beams is expressed by

$$\mathrm{d}f_c = \frac{\partial \mathrm{d}E_c}{\partial y} = \frac{1}{2}(\Delta V_p)^2 \frac{\partial \mathrm{d}C_c}{\partial y} \quad (1)$$

where df_c is the electrostatic coupling force between the two elements, dE_c the energy stored in the capacitor between the two elements, y the total displacement of the elements towards each other along the vibration axis of the resonators, ΔV_p the difference between the two polarization voltages applied to the resonators, and dC_c the value of the coupling capacitor in between the two elements. Each pair of adjacent elements can be considered as a parallel plate capacitor in which the interelectrode gap spacing changes due to the vibrations of the resonators. Assuming small vibration amplitudes compared to the coupling gap size, $\partial \mathrm{d}C_c/\partial y$ is given by:

$$\frac{\partial \mathrm{d}C_c}{\partial y} \approx \frac{\mathrm{d}C_{co}}{g_c}\left(1 + \frac{y}{g_c}\right) \quad (2)$$

where g_c is the coupling gap size in between the resonators, and dC_{co} the rest value of dC_c. Therefore, the electrostatic force can be expressed as:

$$\mathrm{d}f_c = \frac{1}{2}\frac{\mathrm{d}C_{do}(\Delta V_p)^2}{g_c}\left(1 + \frac{y}{g_c}\right) \quad (3)$$

According to Eq. (3), the electrostatic force has a position dependent component (in addition to its constant component) that is in-phase with the displacement of the resonators towards each other (negative electrostatic stiffness). The value of the negative electrostatic stiffness between every two adjacent elements (represented by springs in Fig. 2) is therefore given by:

$$\mathrm{d}K_{elec} = -\frac{\partial \mathrm{d}f_c}{\partial y} = -\frac{(\Delta V_p)^2 \varepsilon h_r \,\mathrm{d}x}{g_c^3} \quad (4)$$

where h_r is the height of the resonators and ε the permitivity of the surrounding environment. This effect is similar to the electrostatic frequency tuning of parallel plate resonators where each electrode adds a negative electrical stiffness to the resonator, reducing its resonant frequency.

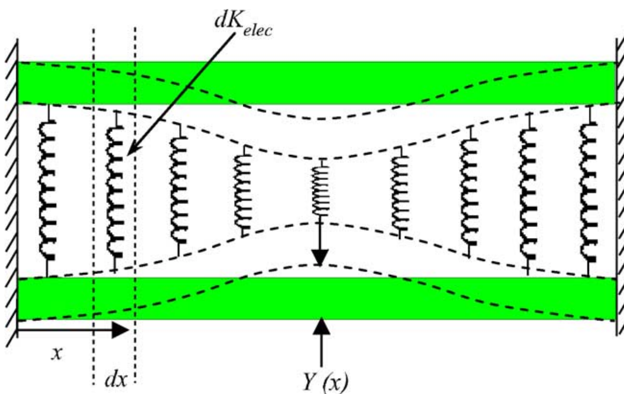

Fig. 2. Schematic diagram of two electrostatically coupled clamped–clamped beam resonators.

3. Electromechanical modeling

3.1. Mechanical lumped-element model

It was shown that the electrostatic force between two adjacent resonators with different polarization voltages is equivalent to a negative mechanical stiffness connecting the two resonators to each other. Similar to mechanical coupling where the resonators are physically connected with compliant mechanical elements, the electrostatically coupled beam resonators are connected by the electrostatic negative stiffness distributed along their length. Therefore the electrostatically coupled filter can be treated as a mechanically coupled filter with a large number of partial coupling elements distributed along the length of the resonators.

For a mechanically coupled second order resonant system, in the first resonance mode the two resonators resonate in-phase at the same frequency as the resonance frequency of the individual resonators and the coupling element has negligible effect in the operation of the filter. In the second

resonance mode, however, the two resonators resonate out-of-phase. Therefore, the coupling element is subject to deformation and adds an extra stiffness to the stiffness of the resonators resulting in a higher frequency resonance mode. Since the deformation of the coupling element is caused by both of the resonators, the added stiffness to each resonator is equivalent to the stiffness of an element with half of the length of the coupling element, i.e. twice the stiffness of the coupling element. The resulting resonance frequency will be:

$$f_1 = f_0\sqrt{1+\frac{2K_c}{K_{r,junc}}} \tag{5}$$

where f_0 is the resonance frequency of individual resonators, K_c the stiffness of the coupling element, and $K_{r,junc}$ the stiffness of the resonators at the position of the coupling element–resonator junction. For narrow-bandwidth filters ($K_c \ll K_{r,junc}$):

$$f_1 - f_0 = \frac{f_0 K_c}{K_{r,junc}} \tag{6}$$

In order to develop a lumped-element mechanical equivalent model for the electrostatically coupled beam filter, the overall effective contribution of all the distributed partial stiffness elements between the beams should be calculated.

According to Eq. (5), the contribution of each partial electrostatic stiffness is determined by the effective stiffness of the resonators at its position. For each beam resonator, the amount of potential energy restored and released in each resonance cycle is:

$$E_p = \frac{1}{2}K_{\mathrm{mech\,eff}}(x)y_{\max^2}(x) \tag{7}$$

where $K_{\mathrm{mech\,eff}}(x)$ is the effective mechanical stiffness, and $y_{\max}(x)$ the resonance amplitude of the beam at position x. Looking at the resonator from different locations along its length, the amount of energy in the resonator is the same while the vibration amplitude changes by location. Consequently the effective stiffness at each location is inversely proportional to the square of the vibration amplitude at that point. Choosing the central point of the beams as the reference position with a vibration amplitude of unity, the effective mechanical stiffness of the beam resonator at its different locations is given by Eq. (8) [7]:

$$K_{\mathrm{mech\,eff}}(x) = \frac{K_{\mathrm{mech\,mid}}}{Y^2(x)} \tag{8}$$

where $Y(x)$ is the normalized mode shape function for the first flexural mode of a clamped–clamped beam resonator having value of unity at the center of the beam.

The effective value of each partial electrostatic coupling element is equivalent to the stiffness resulting in the same frequency separation between the two resonance modes of the filter when placed at the center of the beam and can be calculated using Eq. (9):

$$\mathrm{d}K_{\mathrm{elec\,eff}}(x) = \frac{K_{\mathrm{mech\,mid}}}{K_{\mathrm{mech\,eff}}(x)}\,\mathrm{d}K_{\mathrm{elec}} = Y^2(x)\,\mathrm{d}K_{\mathrm{elec}} \tag{9}$$

Integrating all the partial electrostatic stiffness values along the beam, the overall effective stiffness will be as in Eq. (10):

$$K_{\mathrm{elec\,eff}} = \int_0^L Y(x)^2\,\mathrm{d}K_{\mathrm{elec}} = -\frac{\varepsilon h_r(\Delta V_p)^2}{g_c^3}\int_0^L Y^2(x)\,\mathrm{d}x \tag{10}$$

where $K_{\mathrm{elec\,eff}}$ is equal to the mechanical stiffness resulting in the same resonance mode separation when placed at the center of the beams.

For clamped–clamped beam resonators resonating in their first flexural mode, the normalized mode shape function is [9]:

$$Y(x) = \frac{\cosh(\lambda_1 x/L) - \cos(\lambda_1 x/L) - \sigma_1(\sinh(\lambda_1 x/L) - \sin(\lambda_1 x/L))}{1.588} \tag{11}$$

where λ_1 and σ_1 are constants ($\lambda_1 = 4.73004074$ and $\sigma_1 = 0.982502215$). Integrating the square of the normalized mode shape along the beam length using numerical methods results in $\int_0^L Y(x)^2\mathrm{d}x = 0.39L$.

In the mechanical coupling approach, the coupling strength and consequently the filter bandwidth is determined only by the stiffness and position of the coupling element. As shown by Eq. (10), the coupling strength in electrostatically coupled arrays is a function of the applied polarization voltages as well as the geometrical parameters, i.e. the coupling area and coupling gap size. Therefore the bandwidth of an electrostatically coupled filter can be tuned by changing the polarization voltages to reach the target specifications after the device is fabricated. This tuning capability can be employed to compensate fabrication inaccuracies and temperature drift or implement variable bandwidth filters.

Fig. 3 shows the mechanical equivalent lumped-element model of a second order electrostatically coupled filter and its frequency response. It is worth noting that the mechanical stiffness and mass for the beam resonators in the mechanical model, are the effective stiffness and mass corresponding to the central point of the beams.

The basics of operation and frequency response of the electrostatically coupled resonant systems are the same as their mechanically coupled counterparts. However, unlike the mechanically coupled filters where the resonators move in-phase in the first resonant mode and out-of-phase in the second resonant mode, the resonators are out-of-phase in the first resonance mode of an electrostatically coupled filter, and vice versa. This stems from the fact that the electrostatic coupling spring has a negative effective value and reduces the stiffness

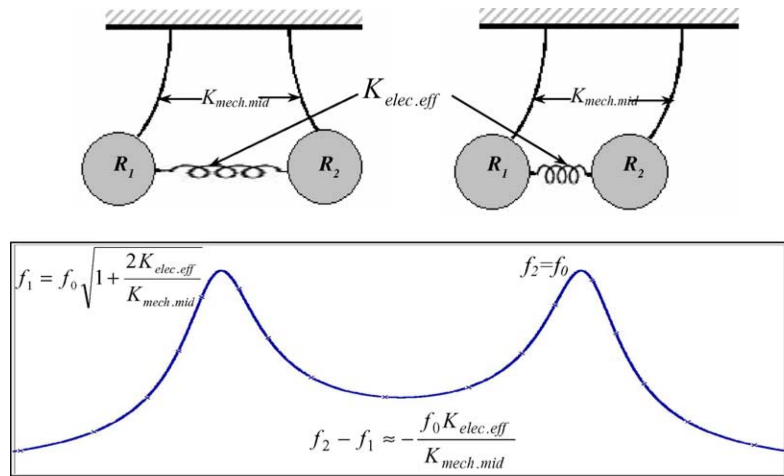

Fig. 3. Equivalent lumped-element model of a second order electrostatically coupled filter and its frequency response.

of the resonator causing a lower frequency resonant mode when interfering with the resonators (in their out-of-phase vibration).

3.2. Electrical equivalent circuit model

To derive an electrical equivalent circuit for the electrostatically coupled filter, the lumped-element mechanical model developed in the previous section is to be converted to its equivalent electrical circuit. The following conversions from mechanical to electrical domain are used:

$$\text{velocity}\,(v) \rightarrow \text{current}\,(i), \qquad \text{force}\,(f) \rightarrow \text{voltage}\,(v)$$

Therefore stiffness is converted to the inverse of capacitance, mass to inductance, and damping to resistance. Since the stiffness, mass and damping element of each resonator have equal velocity (equal current in electrical domain) the resonators are represented by series RLC tanks. The force applied by the coupling stiffness is determined by the sum of the displacements of the resonators. Consequently, the coupling element is to be presented by a parallel negative capacitor to ground at the coupling node in between the two resonators so that the sum of the currents of the resonators determines the voltage of the coupling capacitor.

Based on the discussion above, the electrical equivalent circuit for a second order electrostatically coupled filter is as shown in Fig. 4. The value of the series motional impedance of the resonators (R_{io}, C_{io}, and L_{io}) depends on the mechanical properties of the resonators (mass, stiffness and damping) as well as the electromechanical coupling strength between the input and output electrodes and the resonators. The electromechanical coupling in turn depends on the applied polarization voltages and the capacitive gap between the electrodes and the resonators, as well as the electrode area. The equivalent RLC tank element values for the resonators can be calculated using Eqs. (12)–(14):

$$R_{\text{io}} = \frac{\sqrt{K_{\text{mech mid}} M}\, g_{\text{d}} g_{\text{s}}}{C_{\text{so}} C_{\text{do}} V_{\text{p1}} V_{\text{p2}} Q} \tag{12}$$

$$C_{\text{io}} = \frac{1}{R_{\text{io}} Q \omega_0} = \frac{C_{\text{so}} C_{\text{do}} V_{\text{p1}} V_{\text{p2}}}{\sqrt{K_{\text{mech mid}} M}\, \omega_0 g_{\text{d}} g_{\text{s}}} \tag{13}$$

$$L_{\text{io}} = \frac{1}{C_{\text{io}} \omega_0^2} = \frac{\sqrt{K_{\text{mech mid}} M}\, g_{\text{d}} g_{\text{s}}}{C_{\text{so}} C_{\text{do}} V_{\text{p1}} V_{\text{p2}} \omega_0} \tag{14}$$

where R_{io} is the equivalent motional resistance, Q is the mechanical quality factor of the resonators, C_{so} and C_{do} are the sense and drive electrode capacitances respectively, g_{d} and

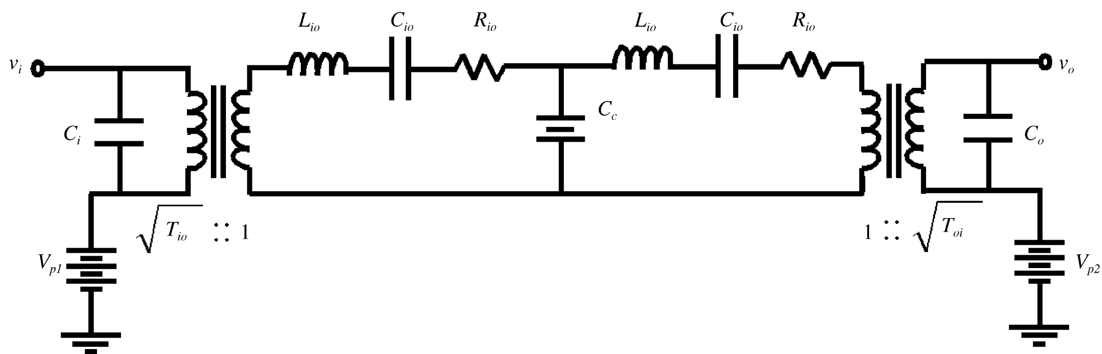

Fig. 4. Electrical equivalent circuit of a second order electrostatically coupled filter.

g_s are the sense and drive capacitive gap sizes, M the equivalent mass of the resonators, and ω_0 is the resonance angular frequency of the resonators.

Since the capacitor values are inversely proportional to the mechanical stiffness they represent, the value of the coupling capacitor will be

$$C_c = \frac{C_{io} K_{\text{mech mid}}}{K_{\text{elec eff}}} \quad (15)$$

Negative effective value of the electrostatic stiffness results in a negative coupling capacitor value.

The two terminating transformers at the input and output of the circuit count for any asymmetry between the input and output ports of the filter which results in different impedance levels at the input and output ports and their transformation coefficients are:

$$T_{io} = \frac{g_s A_d V_{p1}}{g_d A_s V_{p2}} = T_{io}^{-1} \quad (16)$$

Capacitors C_i and C_o at the input and output nodes, represent the physical pad and sense or drive capacitors existing at the input and output of the filter.

The same electrical equivalent circuit can be extended for higher order coupled resonator arrays by adding more resonators and coupling capacitors to the chain. The equivalent circuit parameters will stay the same as given by Eqs. (12)–(16).

Due to the similarity of the electrical equivalent circuits for the capacitively and electrostatically coupled filters, the discussion on insertion loss for electrostatically coupled filters is similar to the capacitively coupled arrays [10].

4. Implementation and verification

4.1. Fabrication

For practical demonstration of the concept of electrostatic coupling, low frequency prototypes of electrostatically coupled beam filters were fabricated on low resistivity SOI substrates. The resonators are fully made of single crystal silicon and are fabricated by patterning the silicon device layer of the SOI substrate to provide isolation between the electrodes and resonators. All features including the transducer sense and drive gaps as well as the coupling gaps were defined by optical lithography and are 1–3 μm wide. High aspect ratio trenches were etched in silicon in an inductively coupled plasma system (ICP) using the Bosch process. The structures were released by removing the underlying oxide layer of the SOI substrate in hydrofluoric acid. Fig. 5 shows the SEM view of a fabricated second order beam filter. The filter consists of two 15 μm thick, 5 μm wide, 500 μm long clamped–clamped beam resonators separated by a 2.8 μm wide coupling gap in between. The capacitive transducer gaps are 1.5 μm wide.

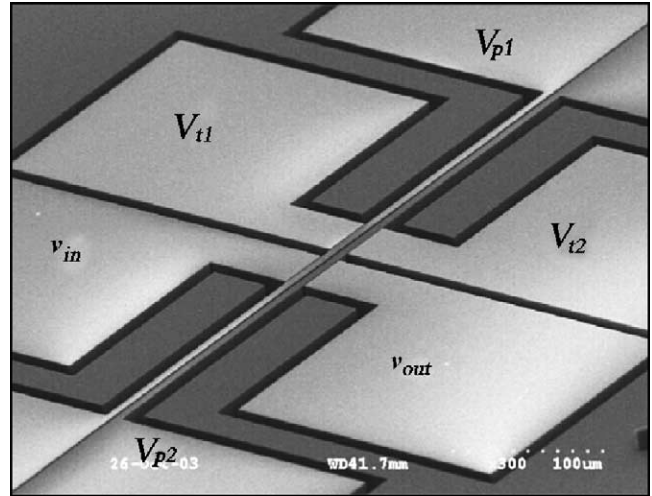

Fig. 5. SEM of a fabricated second order electrostatically coupled clamped–clamped beam filter.

4.2. Measurement

The fabricated filters were tested under vacuum in a custom vacuum system. The schematic diagram of the measurement setup is shown in Fig. 6.

To operate electrostatically coupled filters, different polarization voltages are to be applied to the resonators to provide the electrostatic coupling. On the other hand different polarization voltages cause the resonance frequency of the resonators to have different values while for proper operation of the filter it is required to have equal center frequencies for all the coupled resonators. Therefore, as shown in Fig. 5 tuning electrodes are incorporated in the design of the filter. Application of appropriate tuning voltages to the tuning electrodes induces a slight frequency mismatch between the coupled resonators that is compensated by the polarization voltage difference. The more efficient solution that eliminates the need for tuning electrodes is the application of polarization voltages with opposite polarities and equal absolute values to provide the desired electrostatic coupling while maintaining equal center frequencies.

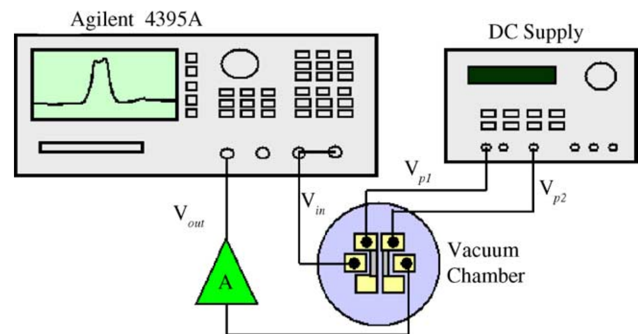

Fig. 6. Schematic diagram of the test setup for characterization of the electrostatically coupled beam filters.

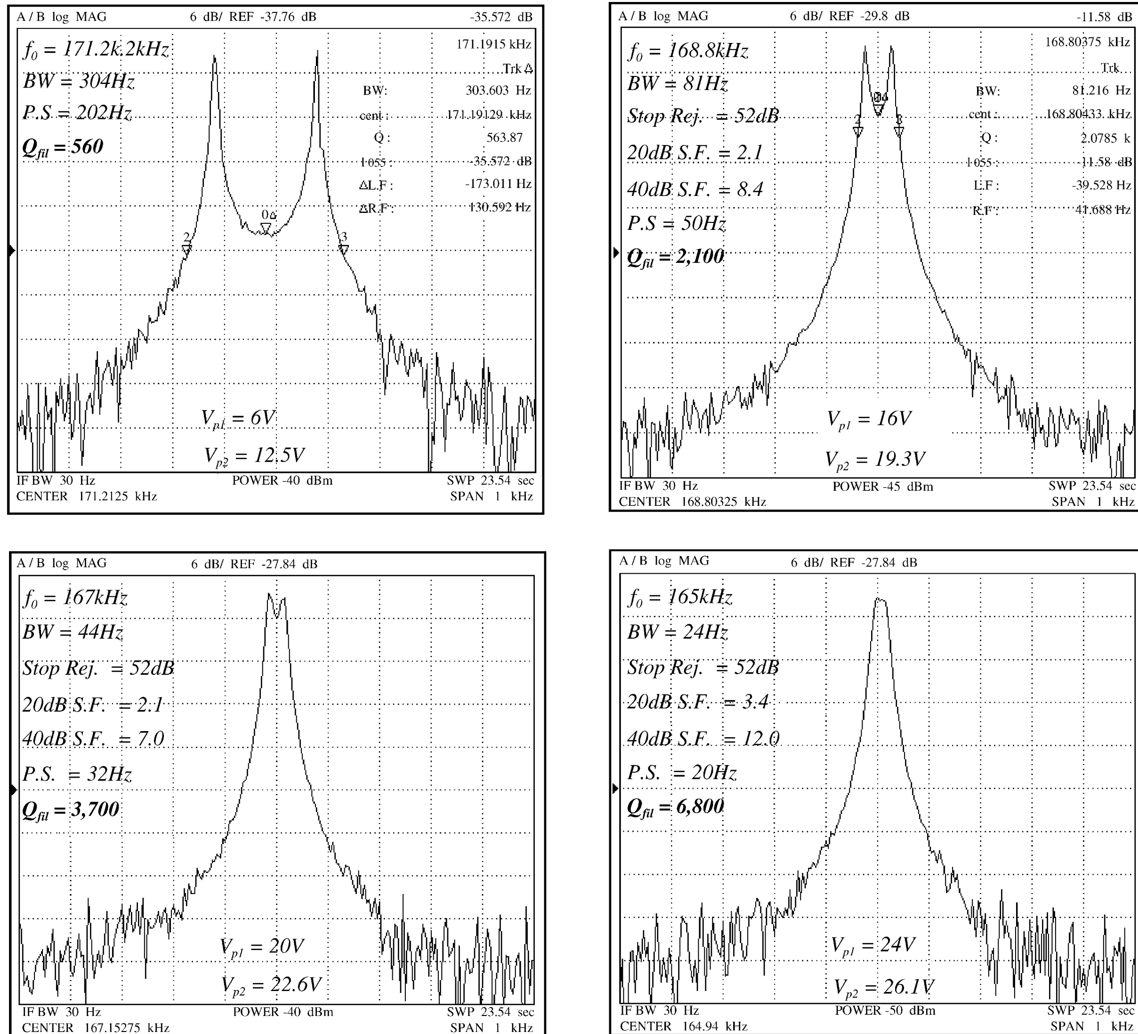

* P.S. = frequency difference between the two resonance modes (peak sepration), Stop Rej. = stopband rejection, and BW = bandwidth.

Fig. 7. Frequency response of the electrostatically coupled filter of Fig. 5 with different sets of polarization voltages applied to the beams.

Fig. 7 shows the frequency responses obtained from the filter of Fig. 5 with different sets of applied polarization voltages. It is worth noting that due to fabrication inaccuracies, there was an intrinsic slight frequency mismatch between the resonance frequencies of the two beams. Therefore filter characteristics were obtained without the need for tuning voltages.

As shown in Fig. 7, filter bandwidth reduces as the value of the applied polarization voltages increases. This can be explained by the fact that the tuning slope of the resonance frequency of a parallel plate resonator is proportional to its polarization voltage:

$$\frac{\partial f}{\partial V_{\mathrm{p}}} = -\frac{V_{\mathrm{p}} f \varepsilon A_{\mathrm{e}}}{K_{\mathrm{mech\,eff}}\, g^{3}} \tag{17}$$

Therefore, as the polarization voltages increase, the frequency tuning slope for the resonators increases and the required polarization voltage difference to compensate the frequency mismatch of the two resonators will be smaller. Smaller polarization voltage difference results in a weaker coupling between the beams and consequently smaller filter bandwidth. Resonance peak separations ranging from 202 to 20 Hz (bandwidth tunability of larger than one decade) were achieved for this filter by changing the polarization voltages. Such tunability is not achievable in any other mechanical or electrical coupling approach. Although a significant bandwidth tuning range was demonstrated for the capacitively coupled filter in Part I of this paper [10], however, bandwidth tuning for such filters is at the cost of change in the filter impedance or its operating frequency. For an electrostatically coupled filter, bandwidth can be tuned by changing the polarization voltage difference between the resonators while maintaining the same DC voltage difference between the resonators and input and output electrodes to avoid frequency or impedance changes.

Filter Q of 6800 and stopband rejection of higher than 50 dB has been achieved for the 24 Hz bandwidth filter of Fig. 7. Quality factor of individual resonators was measured

to be 30,000. Such high filter quality factors cannot be easily achieved for the mechanically coupled filters unless ultra-compliant mechanical coupling elements are employed.

Due to existence of large pad capacitors at the input and output of the device, it was not possible to damp the resonators and flatten the passband by adding resistive terminations. For the same reason insertion loss measurements could not be performed.

4.3. Discussion and verification

The derived equivalent electrical circuit model (Fig. 4) was used for verification of the measured frequency response of the filter. Fig. 8 shows the PSPICE simulation results performed on the equivalent circuit of Fig. 4 with similar polarization voltage values as the measurements. Eqs. (10) and (12)–(15) were used for calculation of the element values in the equivalent circuit. The calculated motional R, L and C as well as the coupling electrostatic stiffness and its equivalent coupling capacitor values for different sets of polarization voltages are presented in Table 1. Excellent agreement between the calculation/simulation results and the measurements confirms the validity of the derived electrical equivalent circuit.

As shown in Table 1, the calculated electrostatic equivalent stiffness values are in the order of 10^{-2} N/m. Such small coupling stiffness values cannot be easily achieved using mechanical coupling elements. Combining Eqs. (6) and (10) results in

$$f_2 - f_1 = -\frac{0.39\varepsilon L_r h_r (\Delta V_p)^2}{g_c^3 K_{\text{mech mid}}} f_0 \tag{18}$$

showing that the frequency difference between the two resonance modes is a linear function of the polarization voltage

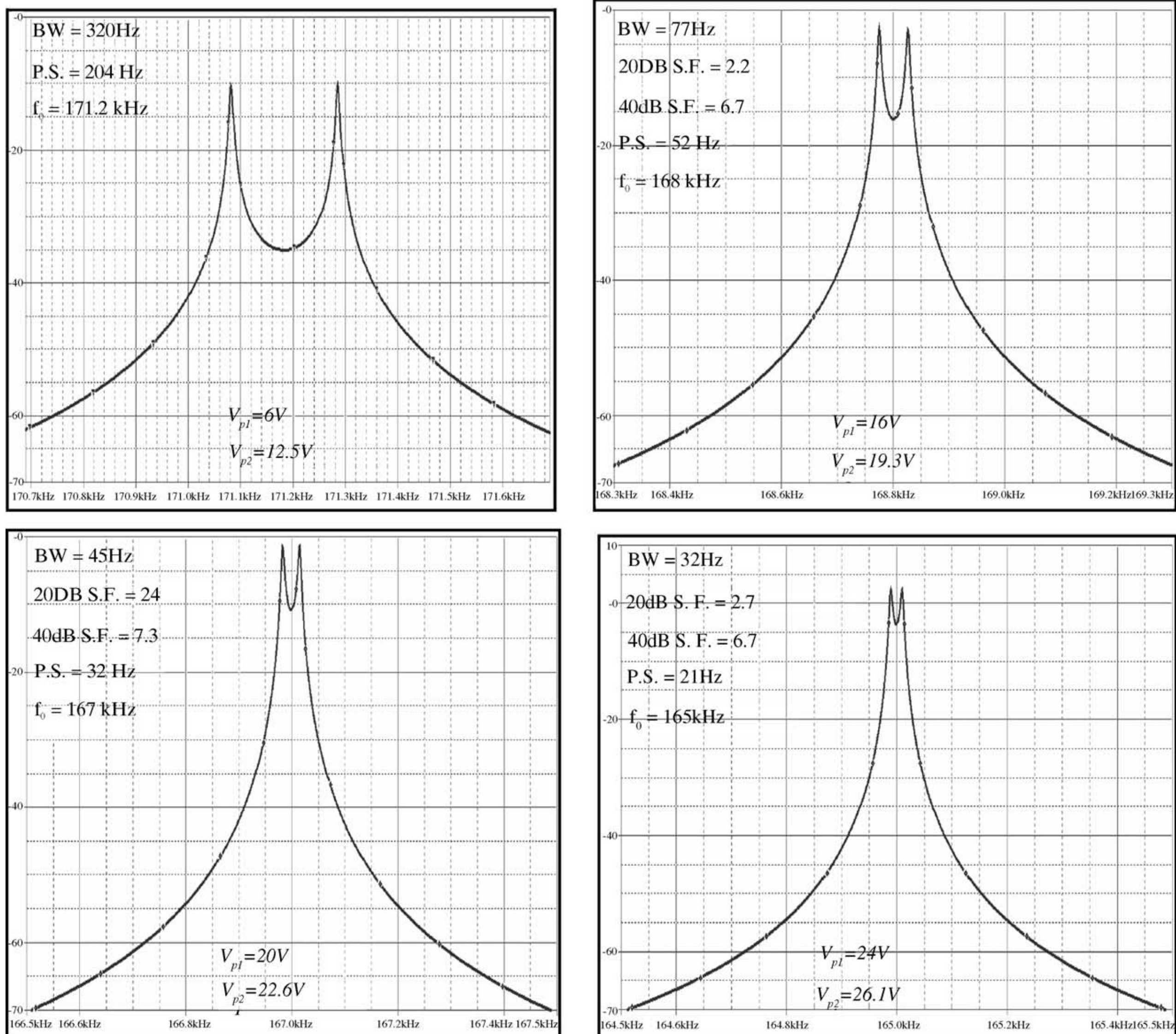

Fig. 8. PSPICE simulation results for the electrostatically coupled filter of Fig. 5 with polarization voltage values similar to the measurement conditions of Fig. 7.

Table 1
Calculated resonator and coupling parameters used in PSPICE simulations of electrostatically coupled filter of Fig. 5 and comparison of simulated/calculated resonance peak separation values with the measured values for different polarization voltages

$K_{r,mid}$ (N/m)	41.81			
$M_{r,mid}$ (ng)	36.17			
R_{io} (MΩ)	3.1	0.753	0.514	0.371
C_{io} (aF)	10.0	41.8	61.8	86.66
L_{io} (H)	86500	21310	14710	10750
K_c (N/m)	−49.8E−3	−12.8E−3	−8.0E−3	−5.2E−3
C_c (fF)	−8.4	−136	−324	−697
V_{p1} (V)	6.0	16.0	20	24.0
V_{p2} (V)	12.5	19.3	22.6	26.1
Calculated/simulated P.S. (Hz)	204	52	32	21
Measured P.S. (Hz)	202	50	32	20

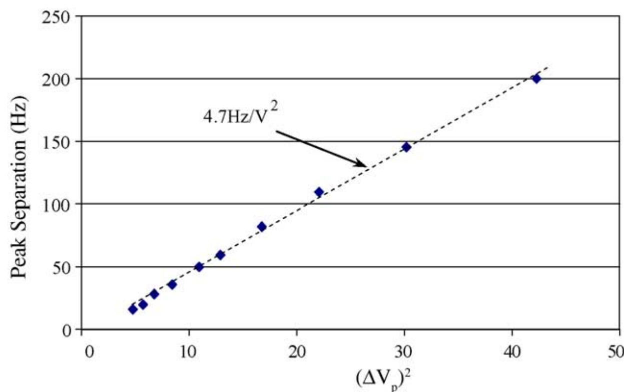

Fig. 9. Resonance peak separation vs. the square of polarization voltage difference (ΔV_p^2) for the electrostatically coupled filter of Fig. 5.

difference squared (ΔV_p^2) and the tuning slope is solely a function of the physical dimensions of the device. The calculated peak separation tuning slope for the 170 kHz filter of Fig. 5 is 4.8 Hz/V^2. Measured values of peak separation for several values of polarization voltage difference as well as the theoretically predicted tuning characteristic with a slope of 4.8 Hz/V^2 are depicted in Fig. 9 showing excellent agreement between the theoretical trend and the measured data. Measured tuning slope extracted from linear extrapolation of the measured data points is 4.95 Hz/V^2.

5. Conclusion

An electrical-based passive coupling technique for implementation of higher order resonant systems from individual micromechanical resonators was introduced. The presented coupling technique is based on electrostatic interaction of closely spaced resonators and does not require any distinct coupling elements. The theoretical derivations and electromechanical modeling of electrostatically coupled beam arrays was presented. It was analytically and practically shown that the coupling strength of electrostatically coupled resonators can be programmed/tuned sharply to the desired bandwidth by adjusting the applied polarization voltages. In addition, compared to mechanically coupled filters, much higher filter quality factors can be achieved for electrostatically coupled filters. Measurement results of a 170 kHz second order electrostatically coupled filter demonstrated filter quality factors as high as 6800 and more than one decade of bandwidth tuning. The same coupling technique can be applied to ultra-stiff bulk-mode resonators for higher frequency operation.

Acknowledgements

This work was supported by DARPA under contract #DAAH01-01-1-R004. The authors would like to thank Gavin Ho and Reza Abdolvand for their contributions and the staff at Georgia Tech Microelectronics Research Center for their assistance.

References

[1] S. Pourkamali, et al., A 600 kHz electrically coupled MEMS bandpass filter, in: Proceedings of the MEMS'03, 2003, pp. 702–705.
[2] A.-C. Wong, et al., Anneal-activated, tunable, 68 MHz micromechanical filters, Sens. Actuators 99 (1999), 1390–1393.
[3] D.S. Greywall, et al., Coupled micromechanical drumhead resonators with practical applications as electromechanical bandpass filters, J. Micromech. Microeng. 12 (2002) 925–938.
[4] R.A. Johnson, Mechanical Filters in Electronics, Wiley/Interscience, 1983.
[5] K. Wang, et al., High-order medium frequency micromechanical electronic filters, JMEMS 8 (4) (1999) 534.
[6] L. Lin, et al., Microelectromechanical filters for signal processing, JMEMS 7 (3) (1998) 286.
[7] K. Wang, et al., Q-enhancement of microelectromechanical filters via low velocity spring coupling, in: Proceedings of the IEEE Ultrasonics Symposium, 1997, pp. 323–327.
[8] S. Pourkamali, et al., Electrostatically coupled micromechanical beam filter arrays, in: Proceedings of the MEMS'04, 2004.
[9] R.D. Blevins, Formulas for Natural Frequency and Mode Shape, Van Nostrand Reinhold, New York, 1979.
[10] S. Pourkamali, F. Ayazi, Electrically coupled MEMS bandpass filters. Part I. With coupling element, J. Sens. Actuators A, in press.

Biographies

Siavash Pourkamali received his BS degree in electrical engineering from Sharif University of Technology, Iran, in 2001 and his MS degree from Georgia Institute of Technology, Atlanta, in 2004. Currently he is pursuing the PhD degree in Electrical Engineering Department, Georgia Institute of Technology. His main research interests are in the areas of RF MEMS resonators and filters, silicon micromachining technologies, and integrated microsystems. He is a 2005 recipient of the Sigma Xi best MS thesis award.

Farrokh Ayazi was born in 19 February 1972. He received his BS degree in electrical engineering from the University of Tehran, Iran, in 1994 and his MS and PhD degrees in electrical engineering from the University of Michigan, Ann Arbor, in 1997 and 2000, respectively. He joined the faculty of Georgia Institute of Technology in December 1999, where he is currently an Assistant Professor in the School of Electrical and Computer Engineering. His current research interests are in the areas of low and high frequency micro- and nanoelectromechanical resonators, VLSI analog integrated circuits, MEMS inertial sensors, and microfabrication technologies. Professor Ayazi is a 2004 recipient of the NSF CAREER award, the 2004 Richard M. Bass Outstanding Teacher Award, and the Georgia Tech. College of Engineering Cutting Edge Research Award for 2001–2002. He received a Rackham Predoctoral Fellowship from the University of Michigan for 1998–1999.